NJC

PAPER

View Article Online
View Journal

Cite this: DOI: 10.1039/c7nj04390b

An auxin–tyrosine derivative based biocompatible supergelator: a template for fabrication of nanoparticles for sustained release of model drugs†

Priyanka Tiwari,[a] Anindya Basu,[b] Sonu Sahu,[b] Sadhna Gound,[b] Ryann M. Christman,[c] Amit K. Tiwari,[c] Piyush Trivedi[b] and Anita DuttKonar *[ab]

Received 12th November 2017,
Accepted 20th February 2018

DOI: 10.1039/c7nj04390b

rsc.li/njc

Bioinspired self-assembling peptides serve as powerful building blocks in the manufacturing of nanomaterials with tailored features. Inspired by the supergelating ability of naphthyl-Phe-OH (hydrogelator **I**), we synthesized naphthyl-Tyr-OH (hydrogelator **II**) and naphthyl-Trp-OH (hydrogelator **III**) with the objective of exploring the propensities of the phenolic OH of Tyr and the NH of the indole for controlling the gelation process. However, our experimental investigation reveals that hydrogelator **II**, containing Tyr as the aromatic core, shows an excellent gelation ability. But the Trp analogue fails to do so under similar conditions. To validate our results we performed MD simulation in an aqueous environment which significantly justifies that hydrogelator **II** exhibits a better hydrogelation ability than hydrogelators **I** and **III**. The characterisation of hydrogelator **II** was then performed in detail using various analytical and microscopic techniques and its biocompatibility was tested using an MTT assay. To examine the potentiality of hydrogelator **II** in drug delivery we developed hydrogel nanoparticles (HNPs) using the concept of self-assembly entirely governed by an ecofriendly approach *i.e.* weak interactions (like H-bonding, π–π and hydrophobic interactions). Our hydrogel nanoparticles display good release kinetics of the model drugs 5-fluorouracil and curcumin from the hydrogel matrix depending on their chemical structure, molecular weight and hydrophobicity. Thus our research shows that the choice of the core residue has a profound impact on the self-assembly process and thus on the gelation properties. Moreover, nanoparticles generated from our novel biocompatible hydrogelator **II** hold promise for future drug delivery applications.

Introduction

Bioinspired self-assembling peptides serve as powerful building blocks in the manufacturing of nanomaterials with tailored features.[1–30] Because of their ease of synthesis, biocompatibility and tunable activity, this emerging class of biomolecules has become very popular.[1–30] To rationally design peptide based low molecular weight hydrogelators (LMOGs), a profound understanding of their gelation mechanism is required. In recent years, many efforts have been made towards investigating the mechanism that drives peptide self-assembly into 3-D matrices. Predicting the likelihood of oligopeptides to form a hydrogel is difficult, as even subtle changes in the molecular architecture may exert a profound impact on its molecular behavior. Although there are no definitive rules for the design of hydrogelators, the existing examples that failed to form hydrogels or successfully gelate may provide insights into the design of oligopeptide-based hydrogelators. Four main forces, Coulomb repulsion, hydrogen bonding, hydrophobicity and π–π interactions, co-operatively interact in guiding peptide self-assembly and thus control the gelation process.[31] To date, although significant examples have been documented, a majority of them consist of longer peptides/peptide amphiphiles as synthons for drug delivery.[32–46] However, the exploration of efficient hydrogels from short peptides/simple amino acid derivatives still remains in its infancy.[47–49]

Henceforth, in this study our aim is to search for simple derivatives with efficient drug delivery abilities. During the investigation process, we found that a series of peptide conjugates possessing polyaromatic protecting groups like fluorenones and phenanthrenes display an excellent hydrogelating ability.[50]

[a] Dept. of Chemistry, Rajiv Gandhi Technological University, Bhopal, India. E-mail: anitaduttkonar@rgtu.net
[b] School of Pharmaceutical Sciences, Rajiv Gandhi Technological University, Bhopal, Airport Bypass Road, Gandhinagar, Bhopal-462033, India
[c] Department of Pharmacology and Experimental Therapeutics, College of Pharmacy and Pharmaceutical Sciences, University of Toledo, OH, USA

† Electronic supplementary information (ESI) available: Details of spectral data, ^{1}H NMR, IR, and mass. See DOI: 10.1039/c7nj04390b

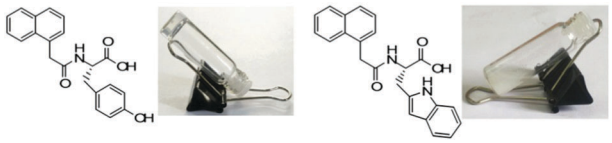

Fig. 1 Chemical structures of hydrogels **II** (left) and **III** (right).

But their major drawback is their carcinogenic nature, thereby restricting their applications in drug delivery.[51,52] Naphthalene is a clinically approved fragment and is present in several drug molecules like propranolol, naphazoline, nafronyl, *etc.*[53–55] So we intend to use this biocompatible and biodegradable fragment naphthyl as our N-terminal protecting group. To ease the burden, few research groups have used this moiety for protection and established their hydrogelation behaviour.[56–59]

Besides, literature documentation has revealed that peptide based hydrogel nanoparticles (NPs) have gained momentum in recent years as a promising drug delivery system.[47–49] This is because of their two different characteristics: (a) hydrophilicity and extremely high water content of hydrogels and (b) exclusively small size of the nanoparticles, which allows them to cross the blood–brain barrier easily and reach the target site. Moreover, amino acid/peptide hydrogel nanoparticles (HNPs) can be modulated rationally by controlling the hierarchical self-assembly process which includes the non-involvement of any potentially hazardous chemicals such as cross-linkers, which may affect their biocompatibility. Also their synthesis procedure is very simple and their *in vivo* degradation products are non-toxic due to the fact that they are composed of simple ecofriendly amino acids.

Thus, inspired by the supergelating ability of a 1-naphthyl Phe[60] derivative, our objectives are (1) to couple the amino acids Tyr and Trp with 1-naphthyl acetic acid, with the idea that the phenolic OH of Tyr and the NH of the indole may enter into additional H-bonding and accentuate the gelation process; (2) to validate our experimental results by MD simulation studies; (3) to characterize the formed gels in detail; and (4) to generate hydrogel nanoparticles from our hydrogelators and explore their implications in drug delivery (Fig. 1). Interestingly, our experimental results reveal that hydrogelator **II** (containing Tyr as the aromatic core) shows an excellent hydrogelation ability. But the Trp analogue fails to do so under similar conditions. Our computational study significantly justifies the experimental observation. The gelation properties of hydrogelator **II** were thoroughly characterized and its biocompatibility was tested using an MTT assay. We further probed the efficiency of this biomolecule as a tool for drug delivery by developing hydrogel nanoparticles (HNPs) using the concept of self-assembly utilizing weak interactions. Our hydrogel nanoparticles display good release kinetics of the model drugs 5-fluorouracil and curcumin from the hydrogel matrix depending on their chemical structure, molecular weight and hydrophobicity.

Results and discussion

Upon addition of 1-Naph-Tyr-OH (hydrogelator **II**) and 1-Naph-Trp-OH (hydrogelator **III**) to water, both gelators dissolved very slowly by the application of a simple heating–cooling cycle. But hydrogelator **II** produced an optically clear gel at room temperature with a MGC of <0.35 mg ml^{-1} almost instantaneously (Fig. 1). But hydrogelator **III** fails to produce a gel, instead forms a translucent viscous aggregate under similar conditions. The gel thus obtained from hydrogelator **II** is stable over a range of pHs, from pH 3.6 to 7 (water), at room temperature and maintains its state for several months. Generally, gelators with MGCs below 0.1% (w/v) fall into the category of supergelators.[61] Therefore our hydrogelator **II** can also be considered as a supergelator. The gelation characterisation of hydrogelator **II** has been dealt with in detail in the subsequent sections.

Computational studies for understanding structures of the hydrogelators

To verify the self-assembling propensities of hydrogelators **I–III** we simulated the geometry optimised structures within an aqueous environment for 10 ps.[62,63] For preliminary understanding of the inter-molecular interactions, only four monomeric units of the hydrogelators were considered. The lowest energy conformers thus obtained are shown in Fig. 2. A recent methodology developed by Ulijn and co-workers is based on thermodynamic stabilization by a self-assembly process, which results in amplification of self-assembling properties and thus accelerates the gelation process.[64]

The sequences of our hydrogelators accommodate short aromatic amino acids: phenylalanine (F), tyrosine (Y) and tryptophan (W) in addition to the naphthyl moiety. So the plausible mechanism of self-assembly in these simple systems is supramolecular β-sheet

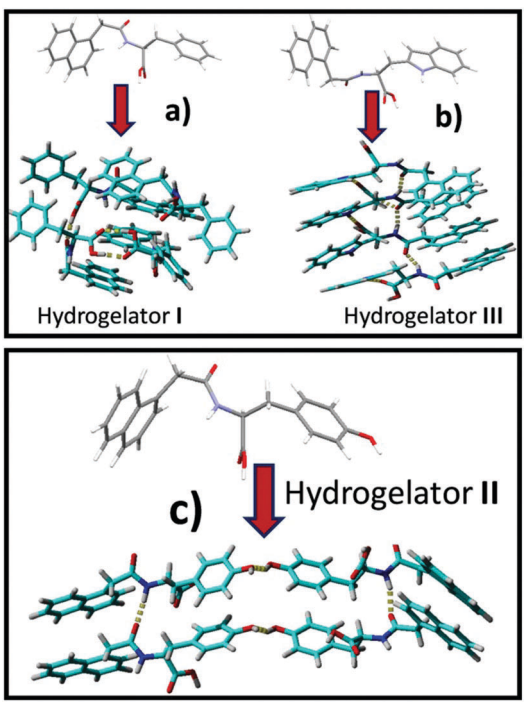

Fig. 2 Energy optimised structures of hydrogelators **I–III** and their self-assembly patterns considering 4 monomeric units.

organization. We expected that a greater involvement of stabilizing interactions amongst the monomers would lead to ordered structures resulting in negative enthalpies of formation. As is evident from the computational studies, the proposed packing model of hydrogelator **I**, containing simple aromatic amino acid side chains, shows the stabilization of a complex β-sheet with the involvement of backbone amides and free carboxylate in intermolecular hydrogen bonding (Fig. 2a). However, insertion of phenolic OH at the *para* position of the aromatic side-chain (Tyr) resulted in an ordered parallel arrangement. Here the H-bonds between Tyr NH and naphthalene amide along with the phenolic OH groups of Tyr confer extra stability to the supramolecular motif (Fig. 2c). This is reflected by the near-ideal peptide bond (dihedral-) angles as observed within the reported conformation (Table S1, ESI†). However, a gradual increase of aromatic steric bulk in the sidechains (from benzyl to indole) results in a parallel β-sheet structure with the involvement of the amide NH of Trp with the carboxylate of 1-naphthoic acid and the NH of the indole. In fact our results indicate that increased participation of the indole NH in H-bond formation may lead to a strain in the planarity of the fused 5-membered ring, where the corresponding dihedral angle can deviate up to 5 degrees or more (Table S1, ESI†). These observations demonstrate that hydrogelator **II** has the highest self-assembling propensity followed by hydrogelators **I** and **III** respectively. This is also evident from the calculated heats of formation of the conformers reported for hydrogelators **I–III**: −945.682, −1819.885 and −281.684 kJ mol^{-1}, respectively. It can therefore be expected that hydrogelator **II**, containing Tyr, exhibits a better ability to rigidify water in comparison to hydrogelator **I**. This premise is in fact in agreement with our experimental observation where the MGC for the Tyr analogue was found to be 0.35 mg ml^{-1} compared to 0.5 mg ml^{-1} for the Phe analogue. Furthermore, in accordance with the much higher heat of formation for hydrogelator **III** we did not observe any gelation properties from the Trp derivative. Thus our simulation studies show that the choice of the core residue has a profound impact on the self-assembly process and thus the gelation properties.

Gel characterisation of hydrogelator II

To evaluate the thermal stability of hydrogelator **II**, gel-to-sol transition temperatures (T_{gel}) were determined (Fig. 3, left) using the ''tube inversion'' method. From the plot it is evident that an increase in the concentration of the gelator (% w/v) leads to an increase in T_{gel} due to enhanced H-bonding and hydrophobic interactions, until a particular concentration is reached. This threshold value signifies the arrival of the saturation limit after which no change in the gel melting temperature occurs (T_{gel}).[65–67]

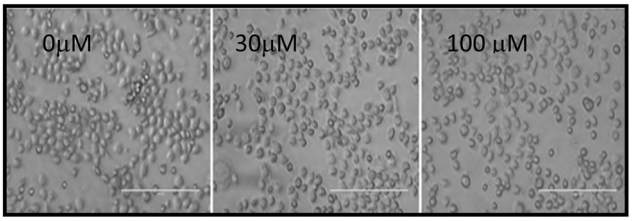

Fig. 4 Morphologies of the cell line OV2008 after treatment with hydrogelators **II**.

To decipher the efficacy of hydrogelator **II** as a vehicle for drug delivery its biocompatibility was tested using *in vitro* cellular experiments.[68] The MTT assay illustrates that hydrogelators **II** tested up to 100 μM did not produce any significant cytotoxicity in all four cell lines HEK293/pcDNA, HCT-116, OV2008 and MDAMB-231 (Fig. 3, right). This investigation was further supported by morphological analysis showcasing no significant cytotoxicity of the hydrogelators (Fig. 4). The higher the IC_{50} values the lower the cytotoxicity and thus the higher the biocompatibility. Therefore, hydrogelators **II** up to 100 μM were determined to be safe in studies for preclinical development.

Our next attempt was to study the secondary structural features of hydrogelator **II**. So we turned to Fourier Transform InfraRed spectroscopy (FT-IR) using the xerogel.

An IR spectrum first shows peaks around 1657 cm^{-1} and 3300 cm^{-1} corresponding to the H-bonded stretching frequencies of the amide carbonyl group and NH respectively. Besides the presence of other peaks around 1732 cm^{-1} (acid carboxylate), 1614 cm^{-1} (amide I) and 1532 (amide II) affirms the presence of a β-sheet conformation in hydrogelator **II** (Fig. S1, ESI†).[69,70]

We then performed morphological analysis using field emission scanning electron microscopy (FE-SEM) using the xerogels obtained from the corresponding hydrogels. Our images (Fig. 5) show the formation of flat nano-fibrillar assemblies with approximately 200 nm width and several micrometres length. These fibres entangled with each other on large length scales to

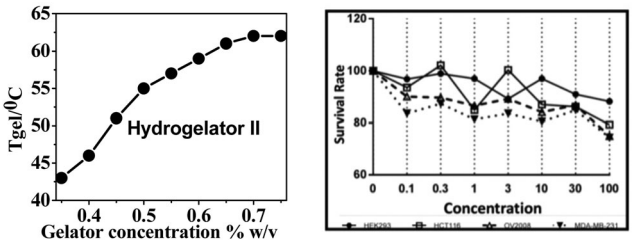

Fig. 3 The change in the T_{gel} profile of hydrogelator **II** (left) and the cell survival study (by MTT assay) of four different cell lines after treatment with hydrogelators **II**.

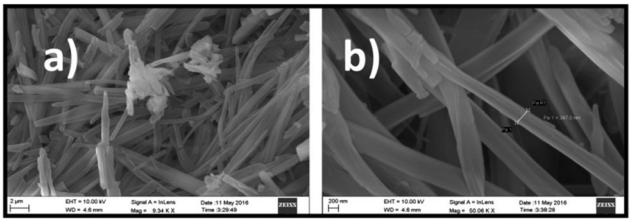

Fig. 5 FESEM images of the xerogel from hydrogelator **II** showing a flat ribbon like morphology of the fibres: (a) lower magnification; and (b) higher magnification.

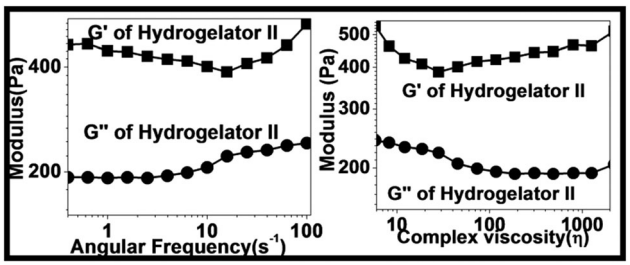

Fig. 6 Rheological study of hydrogel **II** showing variation in G'/G'' with respect to angular frequency (in the left) and complex viscosity (in the right).

form a three dimensional nano-fibrillar network structure, ample enough to entrap water molecules to form a gel.

To determine the mechanical strength and stability of hydrogelator **II**, rheological studies were carried out. In this experiment the storage modulus G' (elastic response) and loss modulus G''(viscous response) were measured against angular frequency.[71–73] As is evident from Fig. 6 (left), throughout the viscoelastic region, the storage modulus (G') is higher than the loss modulus (G'') in the 1 to 100 rad s^{-1} (angular frequency) and 10–1000 eta (complex viscosity) ranges, showing no cross-over point for both cases. This behavior demonstrates a soft gel phase formation. Moreover, this gel matrix bears good tolerance towards external forces. Interestingly, the ratio between G' and G'' of hydrogelator **II** is approximately one order of magnitude higher, denoting significant mechanical stability of the hydrogels. These data prompted us to explore the efficiency of our hydrogel as a drug delivery carrier.

Preparation and characterization of HNPs

It is already known that peptide based hydrogel nanoparticles (HNPs) have attracted attention recently as promising candidates for drug delivery systems owing to their environmentally benign nature.[47–49] Our hydrogelator **II** is biocompatible. So to explore its candidature, we synthesized hydrogel nanoparticles using a modified inverse emulsion process (water-in-oil) as described in Fig. 7a.[47–49] In this experiment an aqueous solution of hydrogelator **II** was gradually added into a solution of vitamin E-TPGS dissolved in light paraffin oil to form a heterogeneous mixture.

This mixture was then homogenized at 30 000 rpm for ten minutes. After this process, the mixture was allowed to self-assemble at 4 °C for 2 h to permit the attachment of the surfactant along the surface of the hydrophilic core (Fig. 7b). Finally, the HNPs were purified using centrifugation. We were able to control the size of the nanoparticles by standardizing the parameters of the emulsion process. Our optimized formulation results reflect that hydrogelator **II** exhibits a bimodal distribution of average particle sizes of 117 ± 21.6 nm and 35.1 ± 5.2 nm (Fig. 7c).[47–49] This bimodal particle size distribution may have resulted due to the equilibrium between two opposite processes, droplet fragmentation and droplet re-coalescence that may have resulted due to the various experimental conditions used in this process, such as surfactant type and the speed of the homogenization.[74] To exemplify our results we performed morphological analysis using TEM-studies. Our TEM images display the presence of two types of well discrete spherical structured nanoparticles, which is in line with the particle size measurement obtained from a zetasizer (Fig. 8a). Moreover, the high −ve value of the zeta potential (−30.8 mV) imparts stability to the formulation.

This negative charge may be due to the presence of carboxylate in the derivative and the surfactant coating around the hydrophobic core.[75,76] Our investigation further shows that the particles have similar diameters and morphologies even after six months, thus emphasizing the stability of the formulation (Fig. 8b).

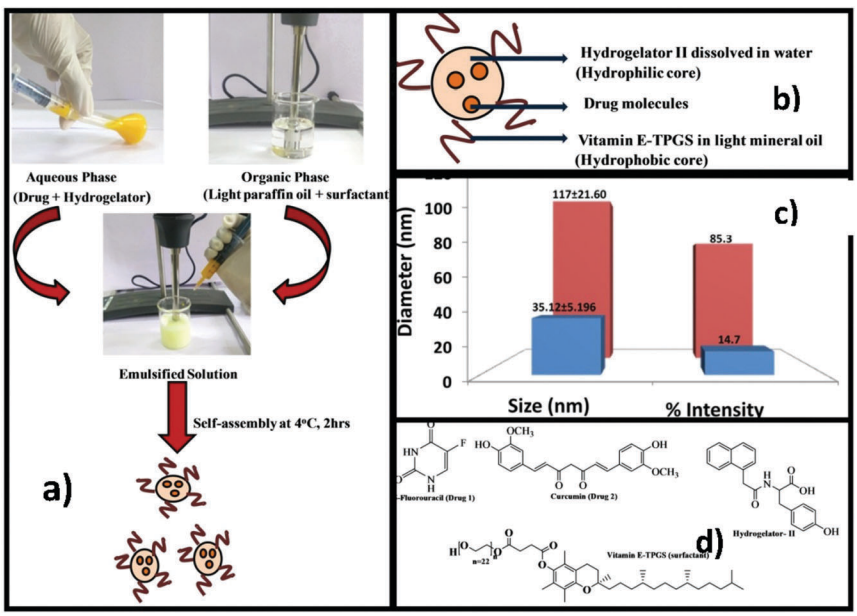

Fig. 7 (a) HNP preparation method, (b) cartoon diagram of the details of a nanoparticle, (c) dimensions of a nanoparticle and (d) structures of the components involved in nanoparticle synthesis.

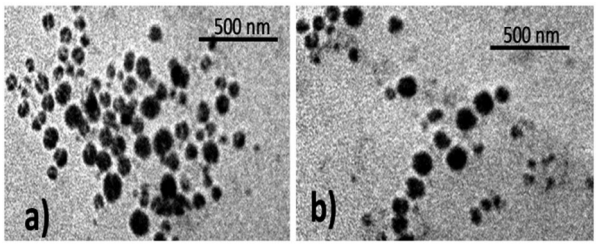

Fig. 8 TEM images of the hydrogel nanoparticles (HNPs) from hydrogelator **II** obtained from the optimized formulation (a) instantaneously (b) after six months.

Drug encapsulation and *in vitro* release studies

Next our attempt was to study the release kinetics of the model drugs 5-fluorouracil and curcumin from the hydrogel matrix using a dialysis membrane as these drugs are known to exhibit chemotherapeutic properties.[47–49,77,78] Moreover, they widely differ in their molecular weight and hydrophobicity. Henceforth, to explore the effects of these characteristics on the release kinetics we chose these two drugs for our studies. The concentrations of the released drugs were measured in solution over time, and quantified using UV spectroscopy in buffer pH 7.45 for 5FU and simulated intestinal medium (SIM) for curcumin at room temperature under gentle stirring conditions.[47–49,76,77] It has been noticed that the release kinetics of 5FU loaded HNPs differ considerably from those of curcumin, which may be because of the difference in their chemical structures, molecular weights and hydrophobicities. The release of 30% of the drug from the HNPs was approximately within 6 h for 5-FU and 10 h for curcumin, respectively, after which the kinetics reached a saturation limit (Fig. 9). We propose that hydrophobic and π–π interactions play a vital role in determining drug release pathways.

Closer inspection of the structures of the drugs shows that 5FU bears groups for H-bonding participation but lacks aromatic units (Fig. 7d). In contrast, curcumin being biphenolic in nature possesses several aromatic moieties apart from H-bond donors and acceptors (Fig. 7d). Our hydrogelator **II** prefers a strand like conformation (Fig. 2c).

In the case of 5-FU (shown in green, Fig. 10), the carboxylates of two strands of hydrogelator **II** first form a dimer between themselves. This entity in turn gets tethered to two 5FU carbonyls by intermolecular H-bonds, with the amide NH of Tyr. Therefore effective drug binding interactions per molecule of naphthyl-Tyr involve one drug molecule per molecule of carrier. But curcumin being bifunctional in nature holds two hydrogelators

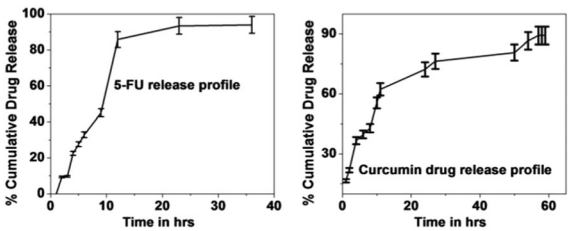

Fig. 9 Release profiles of the model drug from the hydrogel matrix.

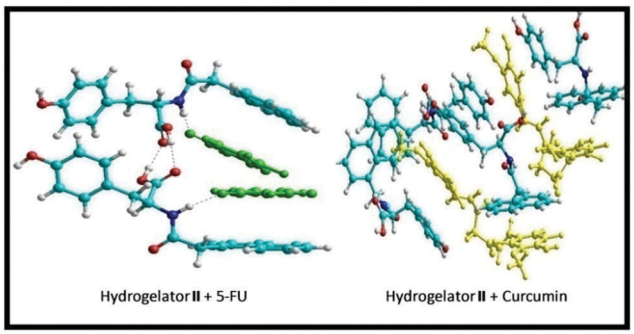

Fig. 10 Geometry optimized structures of 5-FU/curcumin–hydrogelator **II** complexes. All the structures were optimized using the AMBER 99 forcefield. Index of the atom colours – carbon: cyan; hydrogen: white; oxygen: red; nitrogen: blue. The 5FU is coloured green and curcumin yellow for easy differentiation between the hydrogelator and drugs.

from both sides, utilizing π–π and hydrophobic interactions, giving extra stability to the entire system. Therefore, here, per drug molecule, there occur two carriers, which may account for the slower release of curcumin from the hydrogel matrix (Fig. 10).

Conclusions

In summary, in this report we describe the supergelating ability of hydrogelator **II** (containing Tyr as the aromatic core) that rigidifies water at a very low concentration (0.35 mg per ml). But the Trp analogue fails to do so under similar conditions. Our MD simulation studies justify that hydrogelator **II** exhibits a better hydrogelation ability than the others. Furthermore, it also explains why the Trp analogue fails to display a successful gelation ability. Then we characterized in detail hydrogelator **II** using various techniques. We further explored the efficacy of this biomolecule as a tool for drug delivery by developing hydrogel nanoparticles (HNPs) using the concept of self-assembly. To date, literature documentation has revealed that a large number of longer peptides/peptide amphiphiles have been used as synthons for drug delivery systems. However, to the best of our knowledge, our study on hydrogelator **II** represents one of the very few reports of HNP formation emanating from the self-assembly process entirely governed by an eco-friendly approach *i.e.* weak interactions. Our hydrogel nanoparticles display good release kinetics of the model drugs 5-fluorouracil and curcumin from the hydrogel matrix depending on their chemical structure, molecular weight and hydrophobicity. The cause of the slower release of curcumin from the hydrogel matrix has been evidenced by our computational analysis. Thus our research shows that the choice of the core residue has a profound impact on the self-assembly process and thus the gelation properties. Moreover, our novel biocompatible nanoparticles generated from hydrogelator **II** hold promise for drug delivery applications.

Experimental

Materials and methods

Naphthyl 1-acetic acid, 5-fluoro-uracil (5-FU), curcumin and all other chemicals were purchased from Spectrochem. The surfactant

vitamin E-TPGS was purchased from Sigma Aldrich Chemical Company Pvt. Ltd. All solvents used in the synthesis were purified, dried, or distilled, as required. ^{1}H NMR spectra were recorded using a Bruker UltraShield (400 MHz) spectrometer. Mass spectra were recorded in ESI-MS mode on a MicroTOF-Q-II instrument manufactured by Bruker Daltonics; IR spectra were recorded using a Shimadzu Prestige 21 FT-IR spectrometer.

Synthesis of an auxin–amino acid conjugate. Amino acid derivatives were synthesized using a conventional solution phase methodology, with racemization free techniques employing dicyclohexylcarbodiimide (DCC)/(1-hydroxybenzotriazole HOBT) as a coupling agent.[79] Methyl ester hydrochlorides of tyrosine/tryptophan were prepared *via* the thionyl chloride–methanol procedure.[15] All the intermediates obtained were checked for purity by thin layer chromatography (TLC) on silica gel. The final derivatives were purified by column chromatography using silica gel (100–200 meshes) as the stationary phase and an ethyl acetate and petroleum ether mixture as the eluent. The reported derivatives were fully characterised by NMR, IR spectroscopy and mass spectrometry (Scheme 1).

*Naph-Tyr-OMe (**1**).* Tyrosine methyl ester obtained from its hydrochloride (2.12 g, 9.16 mmol) was added to an ice-cooled solution of 1-naphthyl acetic acid (0.682 g, 3.66 mmol) in 4 ml of DMF. Then DCC (1.13 g, 5.49 mmol) was added to the cooled mixture, which was stirred at 1000 rpm approximately for 12 h at room temperature. The progress of the reaction was monitored by TLC. The residue was then taken into ethyl acetate and the DCU (*N*,*N*-dicyclohexylurea) was filtered off. The organic layer was washed with 2 M HCl (3 × 100 ml), 1 M sodium carbonate (3 × 100 ml) and brine (2 × 100 ml), dried over anhydrous sodium sulfate and evaporated in a vacuum to obtain a white solid. The crude peptide was used without further purification.

Yield: 1.33 g, 3.11 mmol (85%); LR-MS: $C_{22}H_{21}NO_4$ $[M]^+$ = 364, M_{calcd} $C_{22}H_{21}NO_4$ $[M]^+$ = 363.

*Hydrogelator **II**.* **1** (1.13 g, 3.11 mmol) was dissolved in 30 ml of MeOH and 1.19 ml of 2 N NaOH was added dropwise to it. The progress of saponification was monitored by thin-layer chromatography (TLC). After 10 h, methanol was removed under vacuum and the residue was taken in 50 ml of water and washed with diethyl ether (2 × 50 ml). The pH of the aqueous layer was then adjusted to 2–3 using 1 N HCl, followed by extraction with ethyl acetate (2 × 50 ml). The extract was pooled, dried over anhydrous sodium sulfate and evaporated *in vacuo* to obtain a white solid.

Yield: 972 mg, 2.78 mmol (90%); m.p. 132–135 °C; FTIR (KBr pellet, cm^{-1}): 3287, 1732, 1657, 1648, 1532, 1513; LR-MS: $C_{21}H_{19}NO_4$ $[M - H]^+$ = 348, M_{calcd} $C_{21}H_{19}NO_4$ $[M]^+$ = 349; ^{1}H NMR (d_6-DMSO, ppm): 9.23 (1H, s, COOH of Tyr), 8.40 (1H, d, NH of Tyr, J = 8.4 Hz), 7.22–7.88 (7H, m, aromatic Hs of the naphthyl ring), 6.96 (2H, d, aromatic Hs of Tyr, J = 8.4 Hz), 6.60 (2H, d, aromatic Hs of Tyr, J = 8.4 Hz), 4.32–4.35 (1H, m, $C^{\alpha}H$ of Tyr), 2.8–2.9 (2H, m, $C^{\beta}Hs$ of Tyr), 2.70–2.76 (2H, m, methylene Hs of naphthyl Grp).

*Hydrogelator-**III**.* Hydrogelator-**III** was synthesized following a similar procedure to that described for hydrogelator-**II**.

Yield: 963 mg, 2.58 mmol (86%); m.p. 137–139 °C; LR-MS: $C_{23}H_{20}N_2O_3$ $[M + H]^+$ = 373, M_{calcd} $C_{23}H_{20}N_2O_3$ $[M]^+$ = 372; FTIR (KBr pellet, cm^{-1}): 3452, 1733, 1719, 1645, 1636, 1530, 1511; ^{1}H NMR (d_6-DMSO, ppm): 10.83 (1H, s, COOH of Trp), 8.46 (1H, d, NH of the indole ring, J = 8 Hz), 7.90–6.92 (13H, m, NH of Trp and aromatic Hs of naphthyl and Trp), 4.51–4.43 (1H, m, $C^{\alpha}H$ of Trp), 3.05–2.98 (4H, m, methylene Hs of naphthyl Grp & $C^{\beta}Hs$ of Trp).

MTT assay. The cytotoxicity of hydrogelator-**II** was determined through MTT (methyl thiazolyl tetrazolium) colorimetric assay, which measures cell metabolic activity through the conversion of tetrazolium dye to insoluble purple formazan crystals as per the method described. The dipeptides were dissolved in DMSO stock solutions followed by making the dilutions (with DMSO $<$0.1%) directly using cell culture media. No precipitation or aggregates were observed even on storage up to 72 hours at 37 °C. The cells were seeded onto flat-bottom 96 well plates at a density of 4000–5000 cells per well. After 24 h, the cells were drugged with serial dilutions (0, 0.1, 0.3, 1, 3, 10, 30, 100 μM) for each of the compounds in triplicate. After 72 h of incubation, MTT dye (4 mg ml^{-1}) was added to all wells and incubated at 37 °C for an additional 4 h. The medium was carefully discarded after this incubation period and formazan crystals were dissolved in 100 μl of DMSO in each well for 15 minutes. Absorbance was measured at a wavelength of 570 nm using a DTX 880 multimode detector (Beckman Coulter Life, Indianapolis, IN, USA). The raw data were analyzed and plotted using GraphPad Prismv7.02. Student's *t*-test was used to analyze all the data.

Field emission scanning electron microscopy study (FESEM). Morphology of xerogels obtained from hydrogelator II were investigated using FESEM microscope (JEOL JSM - 6700F) and were gold coated.

Rheology. Rheological measurements were carried out on a Rheoplus MCR302 (Anton Paar) rotational rheometer with a parallel plate geometry and obtained data were processed with start rheometer software. For oscillatory shear measurements, a parallel top plate with a 25 mm diameter and 1.0 mm gap distance were used. Gels (6 mg ml^{-1}) for rheological experiments were prepared on the bottom plate of the rheometer.

Nanoparticle characterization. The nanoparticle size diameter and surface charge were measured using a Malvern

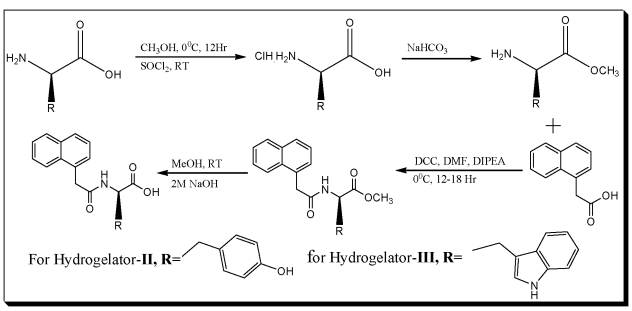

Scheme 1 Synthetic strategy for the preparation of hydrogelators.

Zetasizer, with a 4 mW 633 He–Ne laser (DTS version 4.10, Malvern, U.K.) with appropriate viscosity and refractive index settings. The temperature was maintained at 25 °C during the measurement.

Transmission electron microscopy (TEM). A total of 500 μl of HNPs was prepared and suspended in PBS and placed on a 400-mesh copper grid. After 2 min, the excess of fluid was removed. Negative staining was obtained by covering the grid with 10 μl of 2% uranyl acetate in water. After 2 min, excess uranyl acetate solution was removed. Samples were viewed using a FEI-TECNAI G2 (Netherlands) TEM operating at 200 kV accelerating voltage. Images were acquired digitally using a Gatan CCD camera.

***In vitro* release of drugs from HNPs.** The *in vitro* release profiles of the model drugs 5FU and curcumin from the drug loaded HNPs were obtained using a dialysis membrane previously soaked for 24 h in a dissolution medium and stretched around at one end of the tube. The drug loaded formulations were prepared using pretreated membranes which were immersed into 30 ml of phosphate buffer solution at pH 7.4 for 5-FU and SIM for curcumin at room temperature and magnetically stirred at 50 rpm. At selected time intervals aliquots were withdrawn from the release medium and replaced with the same amount of phosphate buffer (1 ml). The samples were analyzed thrice using a UV-spectrophotometer at 267 nm for 5FU and 432 nm for curcumin. The percentage of cumulative drug release was plotted against time to get the release curves.

Theoretical studies. Expected structures of the designed hydrogelators were computationally compared with that of the Phe derivative. All the molecules under consideration were first geometry optimized, in their respective monomeric forms, using molecular mechanics in the Amber 3 force-field with HyperChem release 8.01.[62,63] Four such monomers were further geometry optimised using the same methodology and the resulting structures obtained were further simulated within an aqueous environment using the Molecular Dynamics (MD) approach. MD simulations were performed using Yasara trial version software, where the desired set of molecules was simulated in a periodic box that extended up to 10 Å on each side with the Amber 99 forcefield. The molecules were simulated at pH 7, 298 K, for at least 10 ps with 1 fs as the time-step and the lowest energy conformer thus obtained during the simulation was reported. The heats of formation of the respective conformers were calculated using the Yasara software and reported.

To study the drug–hydrogelator interactions, the drug molecules and the respective hydrogelators were first geometry optimised individually using the Molecular Mechanics approach, as discussed above. Combinations of the molecules thus obtained were further geometry optimised and the resulting structures were reported.

Conflicts of interest

There are no conflicts of interest to declare.

Acknowledgements

ADK wishes to thank UGC (F.4-(55)/2014(BSR)/FRP), New Delhi, DST (SR/FT/CS-118/2013), New Delhi, and MPCST (A/RD/RP-2/2016-17/58), Govt. of Madhya Pradesh, for financial support. AB is grateful to UGC (F.4-(183)/2014(BSR)/FRP), New Delhi, for financial assistance. All the authors are very much grateful to Dr Sanjit Konar, IISER Bhopal, for his valuable advice. We acknowledge the TEM facility at UGC DAE Consortium for Scientific Research, Indore.

Notes and references

1 S. Zhang, *Nat. Biotechnol.*, 2003, **21**, 1171.
2 M. Reches and E. Gazit, *Curr. Nanosci.*, 2006, **2**, 105.
3 J. J. Panda and V. S. Chauhan, *Polym. Chem.*, 2014, **5**, 4431.
4 E. Busseron, Y. Ruff, E. Moulin and N. Giuseppone, *Nanoscale*, 2013, **8**, 823.
5 B. D. Briggs and M. R. Knetch, *J. Phys. Chem. Lett.*, 2012, **3**, 405.
6 P. Koley and A. Pramanik, *Adv. Funct. Mater.*, 2011, **21**, 4126.
7 A. Sharma, S. Goswami, R. Rajagopalan and A. DuttKonar, *Supramol. Chem.*, 2015, **27**, 625.
8 A. SharmaGangele, S. Goswami, A. Bar, P. Tiwari, S. Konar and A. Dutt Konar, *Cryst. Growth Des.*, 2016, **16**, 2130.
9 A. Dutt, M. G. B. Drew and A. Pramanik, *Tetrahedron*, 2008, **64**, 549.
10 P. Tiwari, R. Verma, A. Sharma and A. Dutt Konar, *ChemistrySelect*, 2018, **3**, 262.
11 A. Sharma, P. Tiwari and A. Dutt Konar, *J. Mol. Struct.*, 2018, **1161**, 44–54.
12 A. Dutt Konar, *J. Mol. Struct.*, 2013, **1036**, 350.
13 A. Dutt Konar, *CrystEngComm*, 2013, **15**, 10569.
14 A. Dutt, M. G. B. Drew and A. Pramanik, *Tetrahedron*, 2005, **61**, 11163.
15 A. Dutt, M. G. B. Drew and A. Pramanik, *Org. Biomol. Chem.*, 2005, **3**, 661.
16 J. M. Chan, L. Zhang, K. P. Yuet, G. Lio, J. W. Rhee, R. Langer and O. C. Farokhzad, *Biomaterials*, 2009, **30**, 1627.
17 A. Dutt Konar, *CrystEngComm*, 2012, **14**, 6689.
18 A. Dutt, A. Dutta, R. Mondal, E. C. Spencer, A. J. K. Howard and A. Pramanik, *Tetrahedron*, 2007, **63**, 10282.
19 S. Ray, A. K. Das and A. Banerjee, *Chem. Mater.*, 2007, **19**, 1633.
20 B. Adhikari, G. Palui and A. Banerjee, *Soft Matter*, 2009, **5**, 3452.
21 A. Dutt, M. G. B. Drew and A. Pramanik, *Org. Biomol. Chem.*, 2005, 2250.
22 E. Gazit, *Chem. Soc. Rev.*, 2007, **36**, 1263.
23 S. Scanlon and A. Agglei, *Nano Today*, 2008, **3**, 22.
24 Y. Yang, U. Khoe, X. Wang, A. Horii, H. Yokoi and S. Zhang, *Nano Today*, 2009, **3**, 22.
25 R. V. Ulijn and A. M. Smith, *Chem. Soc. Rev.*, 2008, **37**, 664.
26 A. Pramanik and D. Haldar, *RSC Adv.*, 2017, **7**, 389.
27 A. M. Jonker, D. W. P. M. Lowik and J. C. M. Van Hest, *Chem. Mater.*, 2012, **24**, 759.

28 Z. M. Yang, G. L. Liang, M. L. Ma, Y. Gao and B. Xu, *J. Mater. Chem.*, 2007, **17**, 850.
29 V. Jayawarna, S. M. Richardson, A. R. Hirst, N. W. Hodson, A. Saiani and J. E. Gough, *Acta Biomater.*, 2009, **5**, 934.
30 J. J. Panda, R. Dua, A. Mishra, B. Mittra and V. S. Chauhan, *ACS Appl. Mater. Interfaces*, 2010, **2**, 2839.
31 L. A. Estroff and A. D. Hamilton, *Chem. Rev.*, 2004, **104**, 1201.
32 M. Suzuki and K. Hanabusa, *Chem. Soc. Rev.*, 2010, **39**, 455.
33 M. Suzuki, C. Setoguchi, H. Shirai and K. Hanabusa, *Chem. – Eur. J.*, 2007, **13**, 8193.
34 A. Baral, S. Roy, A. Dehsorkhi, I. W. Hamley, S. Mohapatra, S. Ghosh and A. Banerjee, *Langmuir*, 2014, **30**, 929.
35 A. Baral, S. Roy, S. Ghosh, D. H. Merino, I. W. Hamley and A. Banerjee, *Langmuir*, 2016, **32**, 1836.
36 N. Nandi, K. Gayen, S. Ghosh, D. Bhunia, S. Kirkham, S. K. Sen, S. Ghosh, I. W. Hamley and A. Banerjee, *Biomacromolecules*, 2017, **18**, 3621.
37 C. K. Thota, N. Yadav and V. S. Chauhan, *Sci. Rep.*, 2016, DOI: 10.1038/Sept 31167.
38 J. Mangelschots, M. Bibian, J. Gardiner, L. Waddington, Y. V. Wanseele, A. V. Eeckhaut, M. M. D. Acevedo, B. V. Mele, A. Madder, R. Hoogenboom and S. Ballet, *Biomacromolecules*, 2016, **17**, 437.
39 K. Basu, A. Baral, S. Basak, A. Dehsorkhi, J. Nanda, D. Bhunia, S. Ghosh, V. Castelletto, I. W. Hamley and A. Banerjee, *Chem. Commun.*, 2016, **52**, 5045.
40 T. Fan, X. Yu, B. Shen and L. Sun, *J. Nanomater.*, 2017, DOI: 10.1155/2017/4562474.
41 D. E. Clarke, E. T. Pashuck, S. Bertazzo, J. V. M. Weaver and M. M. Stevens, *J. Am. Chem. Soc.*, 2017, **139**, 7250.
42 R. V. Rughani and J. P. Schneider, *MRS Bull.*, 2011, **33**, 530.
43 C. Yan, M. E. Mackay, K. Czymmek, R. P. Nagarkar, J. P. Schneider and D. J. Pochan, *Langmuir*, 2012, **28**, 6076.
44 C. Yan, A. Altunbas, T. Yucel, R. P. Nagarkar, J. P. Schneider and D. J. Pochan, *Soft Matter*, 2010, **6**, 5143.
45 S. Zarhitsky and H. Rapaport, *J. Colloid Interface Sci.*, 2011, **360**, 525.
46 L. Mao, H. Wang, M. Tan, L. Ou, D. Kong and Z. Yang, *Chem. Commun.*, 2012, **48**, 395.
47 R. Ischakov, L. A. Abramovich, L. Buzhansky, T. Shekhter and E. Gazit, *Bioorg. Med. Chem. Lett.*, 2013, **21**, 3517.
48 P. Tiwari, R. Ramanathan, M. Moin, R. Soni, P. Trivedi and A. Dutt Konar, *New J. Chem.*, 2017, **41**, 308.
49 P. Tiwari, R. Verma, A. Basu, R. Christmann, D. Waikar, A. K. Tiwari and A. Dutt Konar, *ChemistrySelect*, 2017, **2**, 6623.
50 A. H. Conney, R. L. Chang, D. M. Jerina and S. J. C. Wei, *Drug Metab. Rev.*, 1994, **26**, 125.
51 C. Ioannides, Y. L. Cheung, J. Wilson, D. F. V. Lewis and T. J. B. Gray, *Chem. Res. Toxicol.*, 1993, **6**, 535.
52 M. H. Huang, S. N. Wu, J. P. Wang, C. H. Lin, S. I. Lu, L. F. Liao and A. Y. Shen, *Drug Dev. Res.*, 2003, **60**, 261.
53 Y. B. Rokade and R. Z. Sayyed, *Rasayan J. Chem.*, 2009, **2**, 972.
54 P. Campanoni and P. Nick, *Plant Physiol.*, 2005, **137**, 939.
55 J. Shi, Y. Gao, Z. Yang and B. Xu, *Beilstein J. Org. Chem.*, 2011, **7**(167), 172.
56 G. Liang, Z. Yang, R. Zhang, L. Li, Y. Fan, Y. Kuang, Y. Gao, T. Wang, W. W. Lu and B. Xu, *Langmuir*, 2009, **25**, 8419.
57 Z. Yang, G. Liang, M. M. Y. Gaoa and B. Xu, *J. Mater. Chem.*, 2007, **17**, 850.
58 L. Chen, K. Morris, A. Laybourn, D. Elias, M. R. Hicks, A. Rodger, L. Serpell and D. J. Adams, *Langmuir*, 2010, **26**, 5232.
59 D. J. Adams, K. Morris, L. Chen, L. C. Serpell, J. Bacsaa and G. M. Day, *Soft Matter*, 2010, **6**, 4144.
60 A. Reddy, A. Sharma and A. Srivastava, *Chem. – Eur. J.*, 2012, **18**, 7575.
61 S. Song, L. Feng, A. Song and J. Hao, *J. Phys. Chem. B*, 2012, **116**, 12850.
62 K. C. Bauer, F. Hämmerling, J. Kittelmann, C. Dürr, F. Görlich and J. Hubbuch, *Biotechnol. Bioeng.*, 2017, **114**(4), 821.
63 S. Fraga, J. M. R. Parker and J. M. Pocock, *Computer Simulations of Protein Structures and Interactions*, Springer Berlin Heidelberg, Imprint, Springer, Berlin, Heidelberg, 1995.
64 C. G. Pappas, R. Shafi, I. R. Sasselli, H. Siccardi, T. Wang, V. Narang, R. Abzalimov, N. Wijerathne and R. V. Ulijn, *Nat. Nanotechnol.*, 2016, **11**, 960.
65 J. Naskar, G. Palui and A. Banerjee, *J. Phys. Chem. B*, 2009, **113**, 11787.
66 G. Palui, J. Nanda, S. Ray and A. Banerjee, *Chem. – Eur. J.*, 2009, **15**, 6902.
67 J. Nanda and A. Banerjee, *Soft Matter*, 2012, **8**, 3380.
68 C. Chandrabose, C. Lee, J. Moore, R. Millal, E. A. Suswam, K. L. Abott and S. R. Pondugula, *Bioorg. Med. Chem.*, 2015, **23**, 602.
69 M. Mutter, F. Maser, K. H. Altmann, C. Toniolo and G. M. Bonora, *Biopolymers*, 1985, **24**, 1057.
70 V. Moretto, M. Crisma, G. M. Bonora, C. Toniolo, H. Balaram and P. Balaram, *Macromolecules*, 1989, **22**, 2939.
71 A. Reddy, A. Sharma, Q. Maqbool and A. Srivastava, *RSC Adv.*, 2013, **3**, 18900.
72 A. K. Das, R. Collins and R. V. Ulijn, *Small*, 2008, **4**, 279.
73 A. Dasgupta, J. Hassan Mondal and D. Das, *RSC Adv.*, 2013, **3**, 9117.
74 S. M. Jafari, E. Assadpoor, Y. He and B. Bhandari, *Food Hydrocolloids*, 2008, **22**, 1191.
75 Y. Nagai, L. D. Unsworth, S. Koutsopoulos and S. Zhang, *J. Controlled Release*, 2006, **115**, 18.
76 W. Abdelwahed, G. Degobert, S. Stainmesse and H. Fessi, *Adv. Drug Delivery Rev.*, 2006, **58**, 1688.
77 N. P. Aditya, M. Shim, I. Lee, Y. Lee, M. H. Im and S. Ko, *J. Agric. Food Chem.*, 2013, **61**, 1878.
78 M. L. Bondì, M. R. Emma, C. Botto, G. Augello, A. Azzolina, F. Di Gaudio, E. F. Craparo, G. Cavallaro, D. Bachvarov and M. Cervello, *J. Agric. Food Chem.*, 2017, **66**, 1342.
79 M. Bodanszky and A. Bodanszky, *The Practice of Peptide Synthesis*, Springer-Verlag, New York, 1984, p. 1.

